

# Fast Response Facile Fabricated IDE-Based Ultra-sensitive Humidity Sensor for Medical Applications

Asad Ullah,<sup>||</sup> Muhammad Hamza Zulfqar,<sup>||</sup> Muhammad Atif Khan, Muhammad Zubair,\*  
Muhammad Qasim Mehmood,\* and Yehia Massoud\*



Cite This: *ACS Omega* 2023, 8, 16842–16850



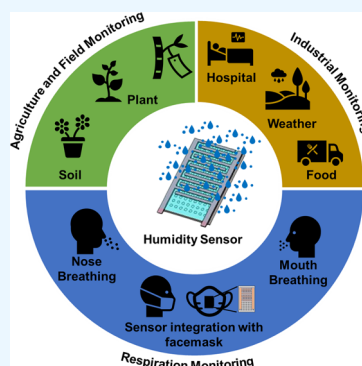
Read Online

ACCESS |

Metrics & More

Article Recommendations

**ABSTRACT:** An eco-friendly, biodegradable, flexible, and facile fabricated interdigital electrode-based capacitive humidity sensor with applications in health and medicine has been reported here. Several sensors use copper tape as electrodes on the polyethylene terephthalate (PET) substrate, with non-woven paper as the sensing layer. Two different configurations of sensors were tested, i.e., with and without pores in the PET substrate. The sensing performance of both sensors has been tested for relative humidity ranging from 35 to 100% at temperatures ranging from 20 to 50 °C. The capacitance of the sensor varies linearly in response to the change in humidity. The sensor with pores shows a response from 28 to 630 pF as the humidity varied from 35 to 100%, whereas the sensor without pores responded from 22 to 430 pF. The response and recovery times of the fabricated sensor are observed as ~2.4, and ~1.8 s, respectively, and the sensitivity is 9.67 pF/% RH. The sensors are tested multiple times, and repeatable results are achieved each time with an accuracy of  $\pm 0.22\%$ . Further, the sensor's response is also stable for different ranges of temperatures. Finally, to demonstrate an application of the proposed sensor, it has been utilized to monitor respiration through nose and mouth breathing. The low-cost, stable, repeatable, and highly sensitive response makes our fabricated sensor a promising candidate for practical field applications.



## 1. INTRODUCTION

Humidity sensors are enormously used to monitor the moisture content or water vapor concentration in the surrounding environment; nowadays, these sensors are used in different fields and commercial applications, including agricultural, food, medical, non-contact sensing, and space applications.<sup>1,2</sup> Different types of humidity sensors have been reported previously depending on their working principles, like resistive, impedance, capacitive, heater, or thermal techniques, and the change observed in their physical parameters after exposure to humidity.<sup>3–5</sup> The most commonly used humidity sensors are resistive or capacitive. Resistance-based sensors have low cost, but the response is non-linear, has low performance, and cannot be used for sensitive applications. On the other hand, capacitive-based sensors are of remarkable interest due to their linear response with high performance and an easy-to-fabricate structure.<sup>6</sup> In a capacitive-based sensor, the sensor's response is observed either by using a parallel plate (PP) design of the sensor or an interdigital electrode (IDE)-based design. In PP sensors, the sensing layer is between the upper and lower electrodes. The sensing material, which is usually a dielectric material, is a vital part of the capacitive sensor, as the response is observed when it interacts with humidity and a change in its dielectric constant occurs. Dielectric materials have a lower dielectric constant value at room temperature than water, which has a dielectric constant value of about 80.<sup>7</sup> IDE-based

capacitive humidity sensors are of great interest in environmental humidity monitoring systems because of their high sensitivity and stable response when their sensing layer absorbs or detects vapor or moisture.<sup>8</sup> The IDE-based sensors are easily fabricated, with comb-shaped metal electrodes patterned on the substrate.<sup>9</sup>

Researchers and scientists strive to enhance the parameters of humidity sensors, like response time, recovery time, physical dependence, temperature effects, sensitivity, linearity, and sensor stability, for long durations.<sup>8</sup> For a single sensor, having the highest values of all these parameters is most likely impossible, so different designs are studied to enhance the parameters. The parameter improvement depends on the materials used in the sensor, mainly the metal electrode and sensing layer. Previous works reported electrodes, like Ag, Au, and Al, and different sensing layers, like two-dimensional materials, hydrophilic polymers, and cellulose paper.<sup>10–14</sup> The response and recovery time associated with operation at high temperatures are challenging for humidity sensors.<sup>15,16</sup>

Received: January 22, 2023

Accepted: April 21, 2023

Published: May 6, 2023



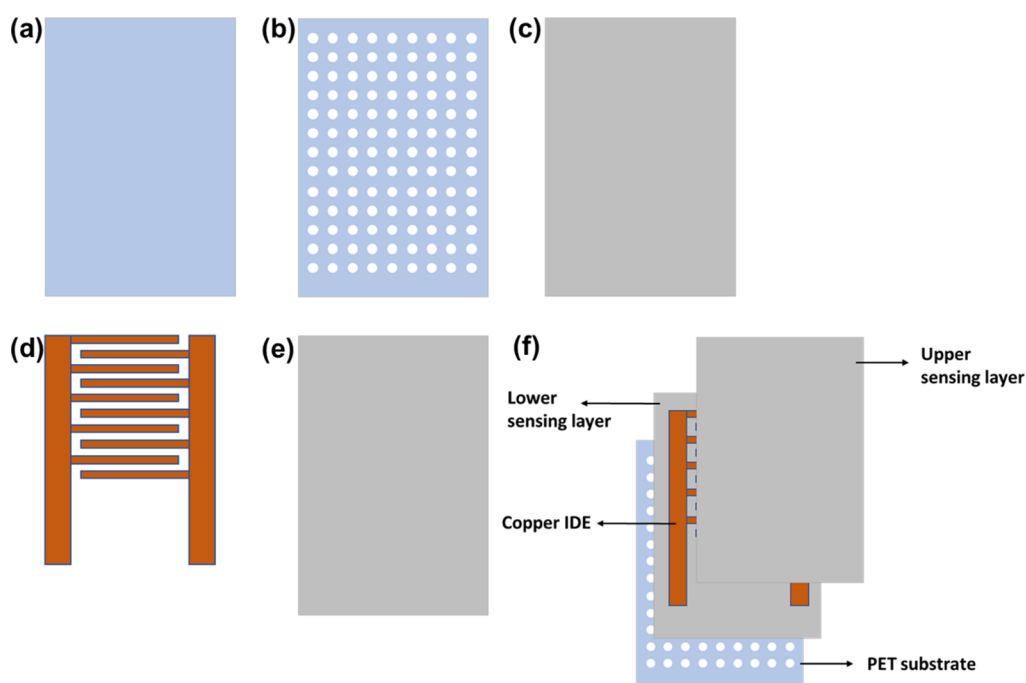


**Figure 1.** IDE capacitive humidity sensor. (a) PET plastic, (b) PET plastic with holes, (c) lower sensing layer non-woven paper, (d) copper electrodes IDE, (e) upper sensing layer non-woven paper, and (f) Fabricated sensor.

Cellulose-based sensors are designed to achieve better response and recovery times. Cellulose is a good moisture absorber because of a hydroxyl group in it; it becomes swollen due to the absorption of humidity.<sup>17</sup> Also, the size of the sensor can play a key role in enhancing parameters like sensitivity, response, and recovery time as large areas are in contact with environmental moisture.<sup>18</sup> But the tradeoff is non-compactness. Recently, studies have been conducted on an array of compact and effective sensors regarding sensitivity, response, and recovery time; the same sensor is replicated.<sup>19</sup>

This paper presents a highly sensitive, flexible, and eco-friendly biodegradable IDE-based humidity sensor using a polyethylene terephthalate (PET) with pores as the substrate, non-woven paper as the sensing layer, and copper tape as electrodes. The sensor is garage-fabricated without any complex and expensive equipment requirements like an inkjet printer, a screen printer, or a gravure printer.<sup>20</sup> Also, the performance of two sensor designs has been compared. These designs are PET substrates with and without pores. The sensing layer is the same for both designs: non-woven paper and copper tape used as electrodes. The response of both the sensors is observed; the one with PET having small pores as a substrate has better response and recovery time with high sensitivity, repeatability, and stability compared to the sensor with normal PET having no pores as the substrate. The sensor with PET as the substrate has the accumulation of capacitance observed above the comb, below the comb, and in between the comb as the humidity is absorbed by the sensing layer from all sides, i.e., from top and bottom. The drawbacks of the sensor with the substrate as a normal PET with no pores are that of its sensitivity and recovery time are not stable from repeatable experiments. It has been attributed that the exposed area that interacts with humidity in normal PET substrate is much smaller than the other. The sensor is tested for the relative humidity range of 35 to 100%, and the response of the sensor in terms of capacitance varies from about 28–650 pF linearly with RH. The response and

recovery times of the sensor are observed as  $\sim 2.5$  and  $\sim 1.8$  s, and the sensitivity is 9.67 pF/% RH. The sensor is also tested for breathing applications. The variation of sensor performance with changing temperatures from 20 to 50 °C is also studied in this work. The effect of temperature on sensor response is negligible, as seen in the experimental result.

## 2. EXPERIMENTAL SECTION

**2.1. Sensor Fabrication and Characterization.** The IDE-based humidity sensor is designed in Corel Draw software with exact dimensions. It is then fabricated using PET with small pores as a substrate, non-woven paper as a sensing layer for both the top and bottom sides, and copper tape as an electrode for both the top and an electrode because of its high electrical conductivity toward humidity. The sensor is garage-fabricated, as simple hands-on fabrication is done without the need for any such complex tools or devices, such as an inkjet printer, gravure printer, screen printing, or spin coating, which makes our sensor cost efficient in terms of electricity savings which are utilized by a fabrication process through these printers.<sup>5,19</sup> The comparison of normal PET and PET with small pores as a substrate is done, and it is experimentally verified that the sensor with the substrate having small pores is highly sensitive compared to the normal PET substrate. Figure 1 shows the fabrication steps of the sensor, with PET having small pores as a substrate. The pores play an important role in the sensitivity because the sensor contact area with humidity is increased by sensing through both the top and bottom sensing layers.

The overall dimension of the sensor is  $L \times W$ , which is 50.8  $\times$  38.1 mm, as shown in Figure 2a, “El” is the electrode length, which is 42 mm, “Ew” is the width of the electrode, which is 5 mm, “Fw” is the width of the comb, which is 2 mm, and “FL” is the length of the comb, which is 2 mm. Copper was used as an electrode because of its highly conductive properties. The gap “g” between the comb is 0.6 cm; the sensor electrode’s dimensions are shown in Figure 2b. The thickness of the

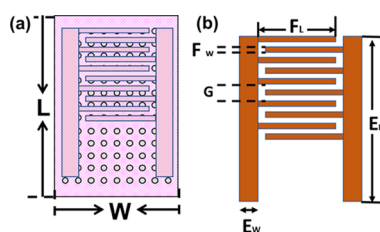


**Figure 2.** Dimensions of the sensor. (a) Overall sensor and (b) copper electrodes IDE.

sensing layer, copper tape, and PET with pores is 0.02, 0.037, and 0.2 mm, respectively. The response of the different dimensions-based sensors was studied by testing, and it was observed that a sensor with a large size is more sensitive than a sensor with a small size because of the large area of the sensor toward moisture. But a very large size is a tradeoff of non-compactness. To deal with such a challenging situation as compactness with better results, we designed a sensor using a double sensing layer above and below a substrate with pores for sensing humidity by the sensing layer. The proposed sensor has acceptable dimensions, high sensitivity, stability, repeatability, and better response and recovery times.

The fabricated sensors are shown in Figure 3. Both sensors are the same in structure and design, as well as in sensing layer and

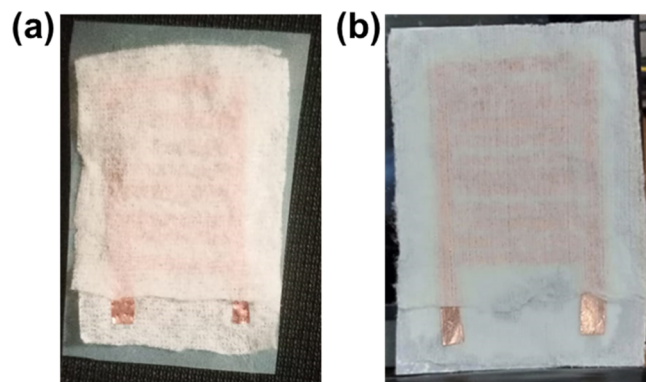


**Figure 3.** Fabricated sensors. (a) PET substrate with pores and (b) PET substrate without pores.

electrodes; the only difference is in the substrate. The sensor's working principle is based on the change in capacitance with a change in humidity. In IDE-based humidity sensors, the capacitance above the sensor comb and in between the comb is of main interest. In our proposed sensor, the capacitance below the comb is also of high interest because the pores in the substrate the water molecules are easily absorbed by the bottom sensing layer, which increases the sensitivity of the sensor.

**2.2. Experimental Setup.** The experimental setup comprises a homemade chamber with a humidifier, dehumidifier, heater, Arduino Mega 2560 board, and reference sensor, as shown in Figure 4. The humidity inside the chamber is controlled through a humidifier, dehumidifier, and heater. The fabricated humidity sensor was integrated with an Arduino Mega 2560 board with analog input ports, and the data were extracted through the serial monitor. The reference sensor, DHT22 sensor, is also integrated with Arduino Mega to compare the results. Through an electric heater, the effect of temperature is studied for different values of temperature. The sensor response is studied, and for comparison, a reference sensor, DHT22, is

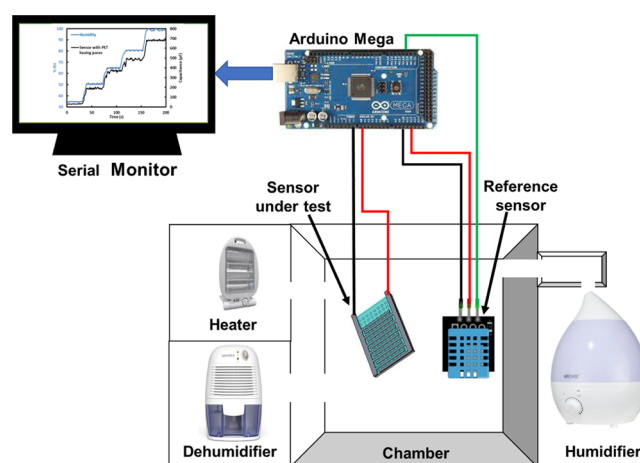


**Figure 4.** Experimental setup for the measurement of humidity.

also used for monitoring humidity and temperature. The relative humidity inside the chamber ranges from 35 to 100% RH, and the temperature varies through the heater from 20 to 50 °C.

**2.3. Working Principle.** The working principle of the sensor and the humidity interaction with the sensor are shown in Figure 5. The sensing layer absorbs the humidity, and the change in capacitance is observed between the finger of the sensor and from both sides, i.e., top and bottom. In most of the previously presented studies about IDE-based humidity sensors, the most concerning capacitance lies on the top and in between the fingers of the sensor. The change in capacitance as humidity changes is the principle of capacitive-based sensors; this phenomenon is explained in the diagram, as shown in Figure 5a. In our proposed sensor, we have designed the IDE sensor in such a way that humidity is exposed to all parts of the sensor easily. As the dielectric constant of water molecules is about 80 at room temperature, which is much higher than that of dielectric material. The higher the concentration of water molecules in the air, the higher the humidity and absorption of the dielectric material from the surrounding area will be. The absorption of the water molecules changes the dielectric constant of the dielectric material,<sup>21</sup> which greatly impacts the capacitance, as capacitance depends on the dielectric constant, number of unit cells, and length of the IDE electrode, as explained by eqs 1 and 2.  $\epsilon$  is the permittivity of the sensing layer,  $\epsilon_1$  is the permittivity of the material between the copper electrodes, and  $\epsilon_2$  is the permittivity of the PET substrate. For the PP-based sensor, the capacitance depends on " $\epsilon_0$ ", which is the dielectric constant of vacuum, " $\epsilon_r$ " is the relative permittivity of the material, " $A$ " is the area, and " $d$ " is the distance between the plates. For increasing the contact of the sensing layer with humidity, we designed an array of meshes in the substrate so that water molecules can be easily absorbed, desorbed, and sensed by the sensing layer from both sides, resulting in a fast change in capacitance, which shows the sensor is highly sensitive toward humidity. The formula for the calculation of capacitance in an interdigitated capacitive based (IDC) sensor is as follows

$$C = C_{UC}(N - 1)L$$

$$C_{UC} = C_u + C_i + C_b$$

$$C_u + C_b = \epsilon_0 \left( \frac{\epsilon + \epsilon_2}{2} \right) \frac{K(\sqrt{1 - (G/W)^2})}{K(G/W)} \quad (1)$$

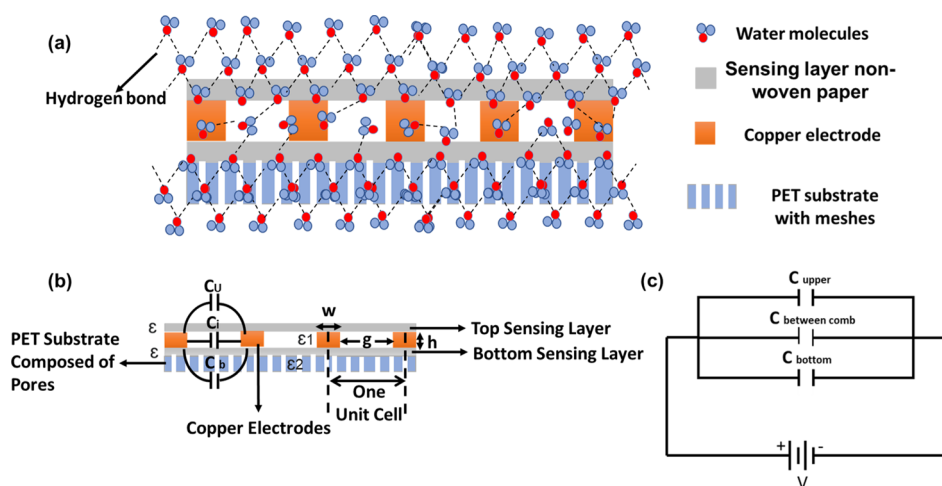


Figure 5. IDE-based sensor. (a) Working and sensing principle, (b) cross-sectional view, and (c) circuit diagram.

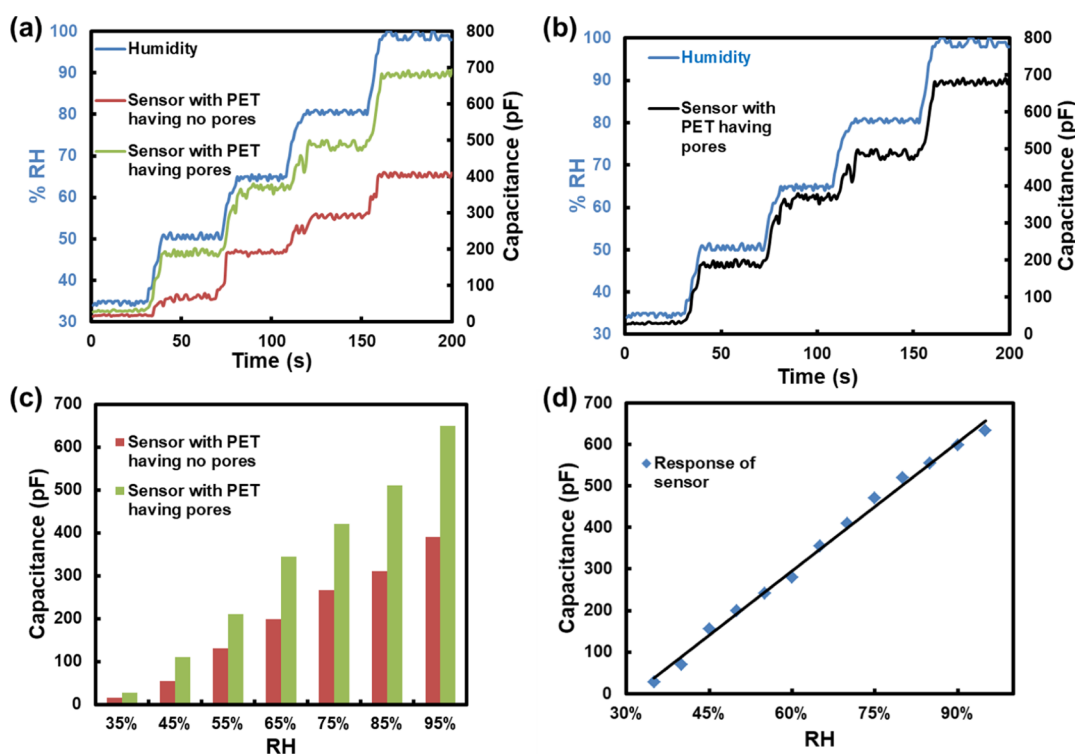


Figure 6. Response of sensors. (a) Using PET substrate with and without pores, (b) Fabricated sensor response with % RH, (c) bars plot at different ranges of humidity for comparison purposes, and (d) linear relationship between capacitance of the sensor with pores and humidity.

$$C_i = \epsilon_0 \epsilon_1 h / G \quad (2)$$

where  $C$  is the capacitance of the IDC sensor,  $C_{UC}$  is the capacitance of a unit cell,  $N$  is the number of unit cells,  $L$  is the length of the sensor electrode,  $G$  is the spacing between the electrodes, and  $W$  is the width of a unit cell, as shown in Figure 3. The capacitance of the IDC sensor increased with the increase in the width of the electrode.

$$C = \epsilon_0 \epsilon_r A / d \quad (3)$$

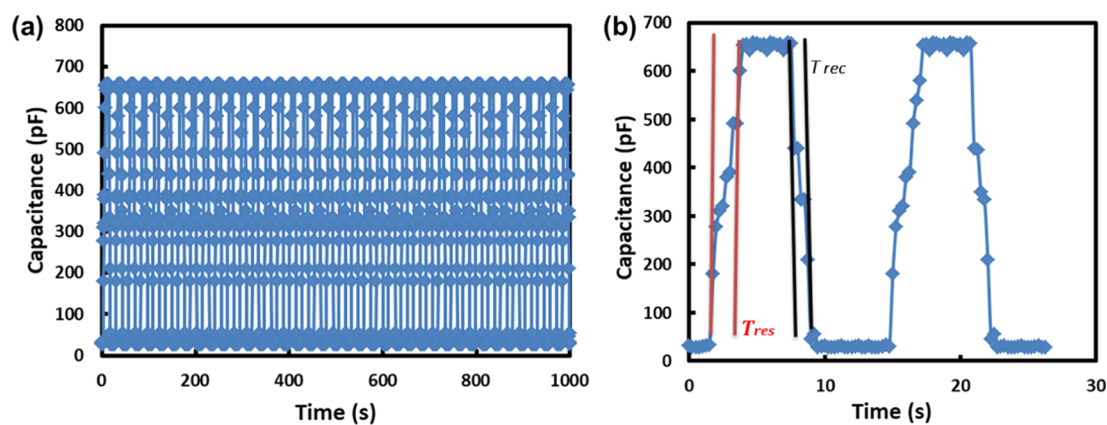
$$C_t = C_u + C_b + C_i \quad (4)$$

Figure 5b,c shows the proposed sensor's cross-sectional view and circuit diagram. In eq 4, " $C_t$ " is the total capacitance of the sensor, which is equal to " $C_u$ ", which is the top capacitance, " $C_b$ " is the bottom capacitance, which is observed due to the bottom

sensing layer absorbing water molecules through pores in the substrate, and " $C_i$ " is the capacitance in between the sensor's fingers/combs. " $W$ " represents the width of the sensor finger, which is 2 mm, " $g$ " is 3 mm, which is the gap between the comb, and " $h$ " is 0.036 mm, which is the height of the electrodes. The sensor is flexible, cost-efficient, biodegradable, has high sensitivity, a stable response, and repeatable results for a longer time.

### 3. RESULTS AND DISCUSSION

The proposed sensor's response toward staircase humidity response and its comparison with normal PET substrate are shown in Figure 6. The results show that the sensor with a PET substrate having small pores is more sensitive than the sensor with PET having no pores. This is because there is less contact



**Figure 7.** Response and recovery of the sensor. (a) Transient and repeatable result for response and recovery and (b) one cyclic response of the sensor.

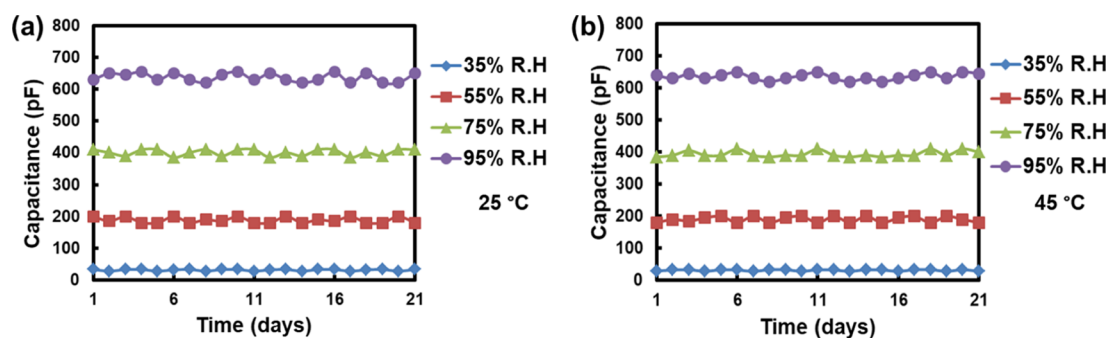


**Figure 8.** Stability and repeatability of the sensor at different values of RH at (a) 25 and (b) 45 °C.

with the sensor's sensing layer from the bottom side, as shown in Figure 6a. Figure 6b shows the fabricated sensor's response. In Figure 6c, the sensor's responses for different humidity levels are shown through a bar graph that differentiates the sensor sensitivity between sensor with and without pores. The sensor is tested multiple times in the chamber for RH ranging from 35 to 100% at normal room temperature. Initially, the capacitance at 35% RH is 28 pF, which increases by increasing the RH through a humidifier. The sensor response is observed for different values of RH, which are 35, 55, 75, and 95%. The sensor response increases for each value of RH as the sensing layer is exposed to humidity. This high increase in response results in high sensitivity of the sensor, repeated experimental results showed a stable and repeatable response of the sensor. A linear response of the sensor with pores is observed, as shown in Figure 6d, through which the determination of RH becomes obvious from the sensor's capacitance.

The important parameters in any field- or commercial-application-based humidity sensor are their response and recovery time. The response and recovery time of the sensor are measured by rapidly changing the RH without equilibrium or delay. A sensor's response time is when 90% of the total capacitance change is achieved during absorption, whereas it takes a sensor's recovery time to achieve 90% of the total capacitance change during desorption.<sup>22</sup> Therefore, we can predict the sensor's sensitivity toward humidity from the response and recovery time. The response time "*T<sub>res</sub>*" and recovery time "*T<sub>rec</sub>*" for our fabricated IDE-based sensor are ~2.5 and ~1.8 s, respectively, as shown in Figure 7b. These values are much better than those from previous work performed using different sensing layers and electrode materials because of the design, we implanted pores in the substrate, due

to which the sensing layers used above and below absorb and desorb the humidity easily.<sup>22</sup> The response and recovery time, which occurs due to the sudden humidification and dehumidification, the humidity is suddenly increased through the humidifier from 35 to 100% and for dehumidification, an electric dehumidifier is used, the response and recovery time is extracted for a short duration from the transient response of the sensor, as shown in Figure 7a, which shows the highly sensitive, stable, and repeatable results. Sensitivity is a key parameter in the design of a humidity sensor which shows the sensor's performance. In most capacitive-based sensors, the sensitivity is affected by higher temperature.<sup>23</sup> In general, the sensitivity of capacitance-based sensors can be calculated using eqs 5 and 6

$$S_c = (\Delta(C)/\Delta(\% RH)) \quad (5)$$

$$S_c = \left( \frac{C_h - C_l}{RH_h - RH_l} \right) \quad (6)$$

where  $C_h$ ,  $C_l$ ,  $RH_h$ , and  $RH_l$  are the highest and lowest values of capacitance and relative humidity of the sensor, which are 650 and 28 pF at 100% RH and 35% RH in our case, respectively.  $\Delta(\% RH)$  is the change between the percentage relative humidity values when measuring values for sensor capacitance. The sensitivity is calculated as 9.67 pF/% RH.

The repeatability and stability tests are performed by placing the sensor in a chamber for consecutively 21 days at different relative humidity values, which are 35, 55, 75, and 95%, and at two different values of temperature, that is, 25 and 45 °C. The repeatable and stable results of the sensor are shown in Figure 8a,b. Temperature has a tremendous effect on humidity sensor, as with an increase in temperature, the kinetic energy of water molecules increases, and therefore the concentration of water

molecules in the air also increases.<sup>24,25</sup> These water molecules when come in contact with the sensor cause an increase in the capacitance of the sensor. Further, the conductance of the electrodes also changes with the temperature, thus causing a change in the performance of the sensor.<sup>26</sup> By keeping in mind these effects, the sensor is tested for different temperature values. The temperature is changed through the heater inside the chamber Figure 9. Shows the response of the sensor for different

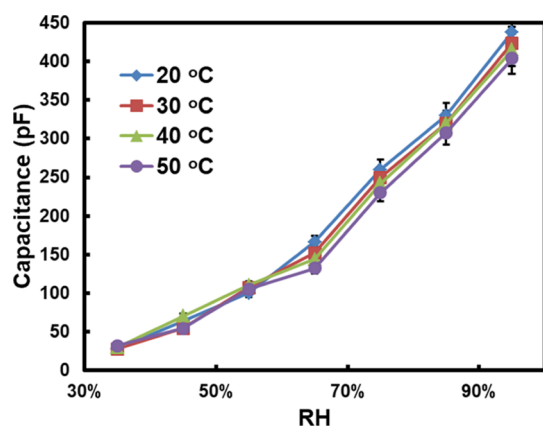


**Figure 9.** Capacitance of the sensor at different values of RH with inset temperatures.

ranges of temperatures. The humidity concentration due to the temperature decrease, but on the other hand, air can easily hold the humidity at higher temperature, which is absorbed by the sensor through the sensing layers. The sensing layer we use in our design is porous and thick, which easily absorbs the water molecules, and the pores in the substrate can help absorb and desorb humidity from the bottom side through, where sensitivity is increased. The pores in PET substrate play an important role in dealing with the temperature effect by enabling higher absorption, unlike sensors with normal PET and PI substrate. In Figure 9, the sensor performance for temperatures of 20, 30, 40, and 50 °C is shown, and for all these temperatures, the response of the sensor is stable. Even the response and recovery time are minutely affected by the temperature. The sensitivity of the sensor for temperatures ranging from 20 to 30 °C saw a minute change of about 0.62% for a temperature range of 30–40 °C, and for a temperature range of 40 to 50 °C, the sensitivity is affected up to 0.32%. The performance of the sensor is barely affected by the temperature. From this result, it is clear that the overall performance of our sensor for a wide range of temperatures is good. The response of the sensor for every 10 °C increase in temperature is affected by up to 1.2%, which is far less than other reports. Our fabricated sensor has advantages in terms of low cost, easy of fabrication, flexibility, and environmental friendliness with repeatable, stable, and highly sensitive performance.

Respiration monitoring using the humidity sensor is one of the fundamental ways to diagnose diseases related to the human body, whether physical or psychological. In recent years, due to the COVID-19 pandemic, the use of non-contact humidity sensors has been in demand for knowing the condition of affected persons. This led scientists and researchers to design a humidity sensor that monitors the breathing rate.<sup>27,28</sup> Also, a TENG-based self-power nanogenerator sensor is designed for breathing monitoring.<sup>29,30</sup> The breathing rate of the human body increases due to physical work load and also due to fear or anxiety.<sup>31</sup> The breathing rate is also different for different ages.

For normal adults, the breathing rate is about 14–20 bpm; for children, about one year of age, the breathing rate is 29–31 bpm. Our proposed sensor is tested for human respiration monitoring, i.e., through nasal and mouth breathing. Figure 10 shows the

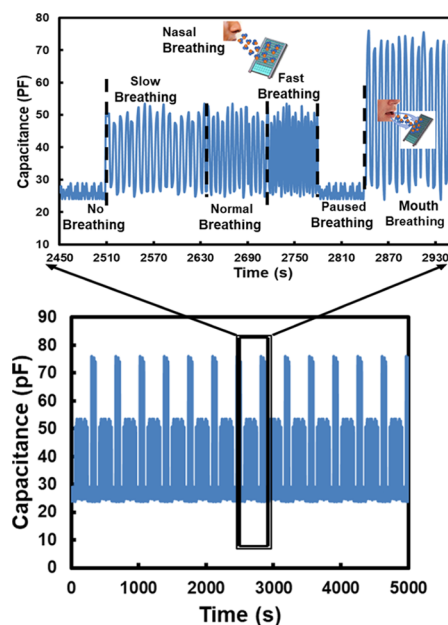


**Figure 10.** Breathing monitoring with no breathing, nasal breathing (slow, normal, and fast), and oral breathing.

sensor response toward no breathing, nasal with slow normal breathing, fast breathing, and mouth breathing. The sensor is found useful for human breath monitoring. At no breathing, the sensor response is about 25–30 pF. During nasal breathing, the sensor response is increased to 45–50 pF, which is lower than oral breathing, which is about 65–70 pF because of the high concentration of humidity in oral breathing.

The response of the sensor is observed through wireless communication on the mobile app using the Bluetooth module and Arduino Mega 2560. The sensor is attached to the inside of the mask in front of the nose. The exhaled air from the nose has a higher concentration of water molecules as compared to air. The response is displayed through the app terminal, stored for each minute, and the breathing is counted after every minute to calculate the breathing rate (Figure 11).

The proposed sensor is eco-friendly and non-hazardous to the environment as it becomes ash after burning, as shown in Figure 12.

Sensor parameters, such as response/recovery time and sensitivity, are compared with other already reported sensors in Table 1. From the table data, it is obvious that our presented sensor exhibits superior performance compared to the previously presented sensor in terms of response/recovery time and sensitivity for the humidity range from 35 to 100% RH.

#### 4. CONCLUSION

This work presents a flexible, highly sensitive, eco-friendly, highly efficient, and low-cost IDE-based humidity sensor. Sensor fabrication is done by using non-woven paper as the sensing layer, copper tape as electrodes, and PET having small pores as the substrate. Sensor performance is observed for the humidity range of 35 to 100% RH and the temperature range of 20 to 50 °C. A humidity chamber with reference sensor DHT22 is used

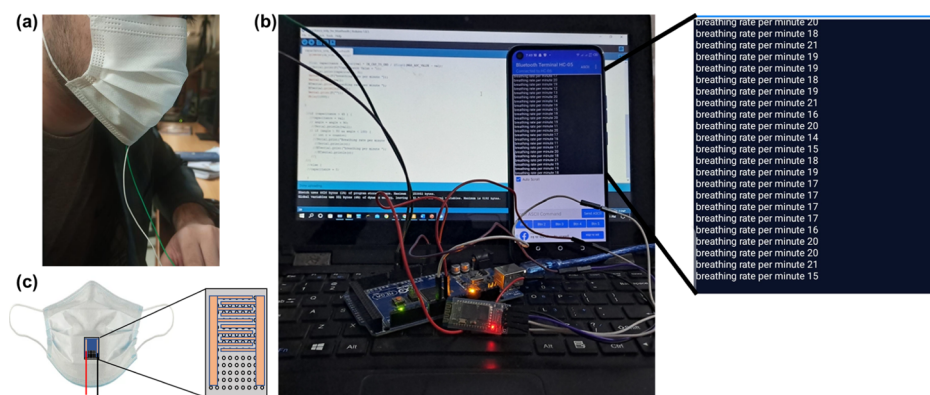


**Figure 11.** Breathing monitoring through wireless communications. (a–c) sensor integrated into the mask. (b) Results displayed through a mobile app.

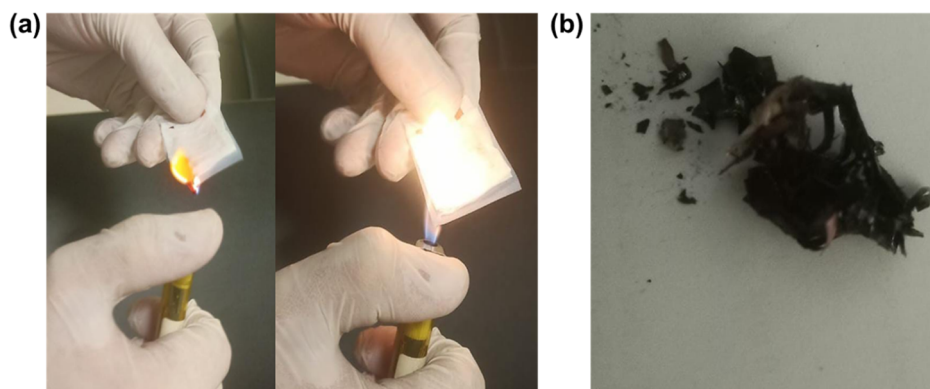


**Figure 12.** Disposal of the sensor. (a) Lighting up sensor and (b) sensor ashes.

**Table 1. Comparison of the Response Time, Recovery Time, and Sensitivity of Different Sensing Materials with Their Sensing Principle**

sensing material	sensing principle	response time	recovery time	sensitivity	humidity range (%)	references
TDTBPPNi metalloporphyrin	capacitive & resistive	35 s	58 s	~102.61 pF/% RH and -333.07 kΩ/% RH	39–85	32
cellulose paper	impedance	25 s	188 s	—	11–95	33
keratin/GO, & keratin/CF	capacitive	39/21 s	80/56 s	633.12 pF/% RH	16–92	34
microporous copper chromite	capacitive	3.6 s	128 s	640 pF/% RH	1–98	35
CNF/CNT	resistive	321 s	435 s	—	11–95	36
CoCr2O4	capacitive	100 s	150 s	70 pF/% RH	5–100	37
A4 paper	resistive	56 s	14 s	—	2–90	38
CAB/PET	capacitive	290 s	193 s	1.2 pF/% RH	20–80	39
origami paper	capacitive	47.3 s	138.6 s	—	10–80	40
PET	resistive	—	—	0.1%/RH	20–80	41
paper	capacitive	250 s	175 s	2 pF/% RH	40–100	42
porous paper (PP)	capacitive	1 min	2–10 min	—	20–100	43
non-woven paper/PET	capacitive	2.4 s	1.8 s	9.67 pF % RH	35–100	this work

for testing the proposed, designed sensor response. The designed sensor with PET having pores as the substrate shows high performance in sensitivity, stability, repeatable results, better response time, and recovery time. This sensor will be efficient in reducing e-waste, which disturbs our environment. Also, this sensor is tested for breath monitoring. Such sensors can be used for various medical, field, and industrial applications.

## ■ AUTHOR INFORMATION

### Corresponding Authors

Muhammad Zubair – *Innovative Technologies Laboratories (ITL), King Abdullah University of Science and Technology*

(KAUST), Thuwal 23955, Saudi Arabia;  
 Email: [muhammad.zubair.3@kaust.edu.sa](mailto:muhammad.zubair.3@kaust.edu.sa)  
 Muhammad Qasim Mehmood – *MicroNano Lab, Department of Electrical Engineering, Information Technology University (ITU) of the Punjab, Lahore S4600, Pakistan;*  
[orcid.org/0000-0002-2793-2137](https://orcid.org/0000-0002-2793-2137);  
 Email: [qasim.mehmood@itu.edu.pk](mailto:qasim.mehmood@itu.edu.pk)  
 Yehia Massoud – *Innovative Technologies Laboratories (ITL), King Abdullah University of Science and Technology (KAUST), Thuwal 23955, Saudi Arabia;*  
 Email: [yehia.massoud@kaust.edu.sa](mailto:yehia.massoud@kaust.edu.sa)

## Authors

Asad Ullah – MicroNano Lab, Department of Electrical Engineering, Information Technology University (ITU) of the Punjab, Lahore 54600, Pakistan

Muhammad Hamza Zulfiqar – Department of Biomedical Engineering, University of Engineering and Technology (UET), Lahore 54890, Pakistan

Muhammad Atif Khan – Innovative Technologies Laboratories (ITL), King Abdullah University of Science and Technology (KAUST), Thuwal 23955, Saudi Arabia

Complete contact information is available at:

<https://pubs.acs.org/10.1021/acsomega.3c00448>

## Author Contributions

<sup>†</sup>A.U. and M.H.Z. contributed equally.

## Notes

The authors declare no competing financial interest.

## ACKNOWLEDGMENTS

The authors would like to acknowledge research funding for the Innovative Technologies Laboratories (ITL) from the King Abdullah University of Science and Technology (KAUST).

## REFERENCES

- (1) Chen, C.; Wang, X.; Li, M.; Fan, Y.; Sun, R. Humidity sensor based on reduced graphene oxide/lignosulfonate composite thin-film. *Sens. Actuators, B* **2018**, *255*, 1569–1576.
- (2) Khan, M. U.; Hassan, G.; Bae, J. J. Bio-compatible organic humidity sensor based on natural inner egg shell membrane with multilayer crosslinked fiber structure. *Sci. Rep.* **2019**, *9*, 5824.
- (3) Duan, Z.; Jiang, Y.; Zhao, Q.; Huang, Q.; Wang, S.; Zhang, Y.; Wu, Y.; Liu, B.; Zhen, Y.; Tai, H. Daily writing carbon ink: novel application on humidity sensor with wide detection range, low detection limit and high detection resolution. *Sens. Actuators, B* **2021**, *339*, 129884.
- (4) Duan, Z.; Zhao, Q.; Wang, S.; Huang, Q.; Yuan, Z.; Zhang, Y.; Jiang, Y.; Tai, H. Halloysite nanotubes: natural, environmental-friendly and low-cost nanomaterials for high-performance humidity sensor. *Sens. Actuators, B* **2020**, *317*, 128204.
- (5) Ullah, A.; Zulfiqar, M. H.; Khan, M. A.; Ali, M.; Zubair, M.; Mehmood, M. Q.; Massoud, Y. Garage-Fabricated, Ultrasensitive Capacitive Humidity Sensor Based on Tissue Paper. *Sensors* **2022**, *22*, 7885.
- (6) Filippidou, M. K.; Chatzichristidi, M.; Chatzandroulis, S. A fabrication process of flexible IDE capacitive chemical sensors using a two step lift-off method based on PVA patterning. *Sens. Actuators, B* **2019**, *284*, 7–12.
- (7) Zouaoui, M. J.; Nait-Ali, B.; Glandut, N.; Smith, D. S. Effect of humidity on the dielectric constant and electrical impedance of mesoporous zirconia ceramics. *J. Eur. Ceram. Soc.* **2016**, *36*, 163–169.
- (8) Ali, S.; Hassan, A.; Hassan, G.; Bae, J.; Lee, C. H. All-printed humidity sensor based on Graphene/methyl-red composite with high sensitivity. *Carbon* **2016**, *105*, 23–32.
- (9) Khan, M. U.; Saqib, Q. M.; Hassan, G.; Bae, J. All printed organic humidity sensor based on egg albumin. *Sensing Bio-Sensing Res.* **2020**, *28*, 100337.
- (10) Awais, M.; Khan, M. U.; Hassan, A.; Bae, J.; Chattha, T. E. Printable highly stable and superfast humidity sensor based on two dimensional molybdenum diselenide. *Sci. Rep.* **2020**, *10*, 5509–5513.
- (11) Cichosz, S.; Masek, A.; Zaborski, M. Polymer-based sensors: A review. *Polym. Test.* **2018**, *67*, 342–348.
- (12) Li, Z.; Wang, J.; Xu, Y.; Shen, M.; Duan, C.; Dai, L.; Ni, Y. Green and sustainable cellulose-derived humidity sensors: A review. *Carbohydr. Polym.* **2021**, *270*, 118385.
- (13) Yan, W.; Zhang, D.; Liu, X.; Chen, X.; Yang, C.; Kang, Z. Guar gum/ethyl cellulose-polyvinyl pyrrolidone composite-based quartz

crystal microbalance humidity sensor for human respiration monitoring. *ACS Appl. Mater. Interfaces* **2022**, *14*, 31343–31353.

- (14) Wang, D.; Zhang, D.; Li, P.; Yang, Z.; Mi, Q.; Yu, L. Electrospinning of flexible poly (vinyl alcohol)/MXene nanofiber-based humidity sensor self-powered by monolayer molybdenum diselenide piezoelectric nanogenerator. *Nano-Micro Lett.* **2021**, *13*, 57.
- (15) Shinde, P. V.; Saxena, M.; Singh, M. K. Recent developments in graphene-based two-dimensional heterostructures for sensing applications. *Fundam. Sens. Appl. 2D Mater.* **2019**, 407–436.
- (16) Li, X.; Wang, Y.-H.; Zhao, C.; Liu, X. Paper based piezoelectric touch pads with hydrothermally grown zinc oxide nanowires. *ACS Appl. Mater. Interfaces* **2014**, *6*, 22004–22012.
- (17) Dai, L.; Wang, Y.; Zou, X.; Chen, Z.; Liu, H.; Ni, Y. Ultrasensitive physical, bio, and chemical sensors derived from 1-, 2-, and 3-D nanocellulosic materials. *Small* **2020**, *16*, 1906567.
- (18) Duan, L.; D'hooge, D. R.; Cardon, L. Recent progress on flexible and stretchable piezoresistive strain sensors: From design to application. *Prog. Mater. Sci.* **2020**, *114*, 100617.
- (19) Zhou, L.; Wang, M.; Liu, Z.; Guan, J.; Li, T.; Zhang, D. High-performance humidity sensor based on graphitic carbon nitride/polyethylene oxide and construction of sensor array for non-contact humidity detection. *Sens. Actuators, B* **2021**, *344*, 130219.
- (20) Delipinar, T.; Shafique, A.; Gohar, M. S.; Yapici, M. K. Fabrication and materials integration of flexible humidity sensors for emerging applications. *ACS Omega* **2021**, *6*, 8744–8753.
- (21) Kulwicki, B. M. Humidity sensors. *J. Am. Ceram. Soc.* **1991**, *74*, 697–708.
- (22) Arunachalam, S.; Izquierdo, R.; Nabki, F. Low-hysteresis and fast response time humidity sensors using suspended functionalized carbon nanotubes. *Sensors* **2019**, *19*, 680.
- (23) El-Denglawey, A.; Manjunatha, K.; Sekhar, E. V.; Chethan, B.; Zhuang, J.; Angadi, J. Rapid response in recovery time, humidity sensing behavior and magnetic properties of rare earth (Dy & Ho) doped Mn–Zn ceramics. *Ceram. Int.* **2021**, *47*, 28614–28622.
- (24) Islam, T.; Uddin, Z.; Gangopadhyay, A. Temperature effect on capacitive humidity sensors and its compensation using artificial neural networks. *Sens. Transducers* **2015**, *191*, 126.
- (25) Mogera, U.; Sagade, A. A.; George, S. J.; Kulkarni, G. U. Ultrafast response humidity sensor using supramolecular nanofibre and its application in monitoring breath humidity and flow. *Sci. Rep.* **2014**, *4*, 4103–4109.
- (26) Gaspar, C.; Olkkonen, J.; Passoja, S.; Smolander, M. Paper as active layer in inkjet-printed capacitive humidity sensors. *Sensors* **2017**, *17*, 1464.
- (27) Wang, Y.; Zhang, L.; Zhang, Z.; Sun, P.; Chen, H. High-sensitivity wearable and flexible humidity sensor based on graphene oxide/non-woven fabric for respiration monitoring. *Langmuir* **2020**, *36*, 9443–9448.
- (28) Wang, D.; Zhang, D.; Chen, X.; Zhang, H.; Tang, M.; Wang, J. Multifunctional respiration-driven triboelectric nanogenerator for self-powered detection of formaldehyde in exhaled gas and respiratory behavior. *Nano Energy* **2022**, *102*, 107711.
- (29) Liu, X.; Zhang, D.; Wang, D.; Li, T.; Song, X.; Kang, Z. A humidity sensing and respiratory monitoring system constructed from quartz crystal microbalance sensors based on a chitosan/polypyrrole composite film. *J. Mater. Chem. A* **2021**, *9*, 14524–14533.
- (30) Wang, D.; Zhang, D.; Guo, J.; Hu, Y.; Yang, Y.; Sun, T.; Zhang, H.; Liu, X. Multifunctional poly (vinyl alcohol)/Ag nanofibers-based triboelectric nanogenerator for self-powered MXene/tungsten oxide nanohybrid NO<sub>2</sub> gas sensor. *Nano Energy* **2021**, *89*, 106410.
- (31) Boiten, F. A.; Frijda, N. H.; Wientjes, C. J. Emotions and respiratory patterns: review and critical analysis. *Int. J. Psychophysiol.* **1994**, *17*, 103–128.
- (32) Farooq, Z.; Yaseen, M.; Zulfiqar, M.; Mahmood, M. H. R.; Akram, R.; Qadir, K. W.; Zafar, Q. Investigation of relative humidity-sensing performance of capacitive and resistive type sensor based on TDTBPPNi metalloporphyrin dielectric layer. *Bull. Mater. Sci.* **2021**, *44*, 156–210.



(33) Guan, X.; Hou, Z.; Wu, K.; Zhao, H.; Liu, S.; Fei, T.; Zhang, T. Flexible humidity sensor based on modified cellulose paper. *Sens. Actuators, B* **2021**, *339*, 129879.

(34) Hammouche, H.; Achour, H.; Makhlof, S.; Chaouchi, A.; Laghrouche, M. A comparative study of capacitive humidity sensor based on keratin film, keratin/graphene oxide, and keratin/carbon fibers. *Sens. Actuators, A* **2021**, *329*, 112805.

(35) Mahapatra, P. L.; Das, S.; Mondal, P. P.; Das, T.; Saha, D.; Pal, M. Microporous copper chromite thick film based novel and ultrasensitive capacitive humidity sensor. *J. Alloys Compd.* **2021**, *859*, 157778.

(36) Zhu, P.; Ou, H.; Kuang, Y.; Hao, L.; Diao, J.; Chen, G. Cellulose nanofiber/carbon nanotube dual network-enabled humidity sensor with high sensitivity and durability. *ACS Appl. Mater. Interfaces* **2020**, *12*, 33229–33238.

(37) Mahapatra, P. L.; Mondal, P. P.; Das, S.; Saha, D. Novel capacitive humidity sensing properties of cobalt chromite nanoparticles based thick film. *Microchem. J.* **2020**, *152*, 104452.

(38) Duan, Z.; Jiang, Y.; Zhao, Q.; Huang, Q.; Wang, S.; Zhang, Y.; Wu, Y.; Liu, B.; Zhen, Y.; Tai, H. Daily writing carbon ink: novel application on humidity sensor with wide detection range, low detection limit and high detection resolution. *Sens. Actuators, B* **2021**, *339*, 129884.

(39) Zhang, Z.; Chen, M.; Alem, S.; Tao, Y.; Chu, T. Y.; Xiao, G.; Ramful, C.; Griffin, R. Printed flexible capacitive humidity sensors for field application. *Sens. Actuators, B* **2022**, *359*, 131620.

(40) Chen, X.; Li, Y.; Wang, X.; Yu, H. Origami Paper-Based Stretchable Humidity Sensor for Textile-Attachable Wearable Electronics. *ACS Appl. Mater. Interfaces* **2022**, *14*, 36227–36237.

(41) Turkani, V. S.; Narakathu, B. B.; Maddipatla, D.; Bazuin, B. J.; Atashbar, M. Z. P1FW. 5-A fully printed CNT based humidity sensor on flexible PET substrate. *Proc. IMCS* **2018**, 519–520.

(42) Gaspar, C.; Olkkonen, J.; Passoja, S.; Smolander, M. Paper as active layer in inkjet-printed capacitive humidity sensors. *Sensors* **2017**, *17*, 1464.

(43) Niarchos, G.; Dubourg, G.; Afroudakis, G.; Georgopoulos, M.; Tsouti, V.; Makarona, E.; Crnojevic-Bengin, V.; Tsamis, C. Humidity sensing properties of paper substrates and their passivation with ZnO nanoparticles for sensor applications. *Sensors* **2017**, *17*, 516.